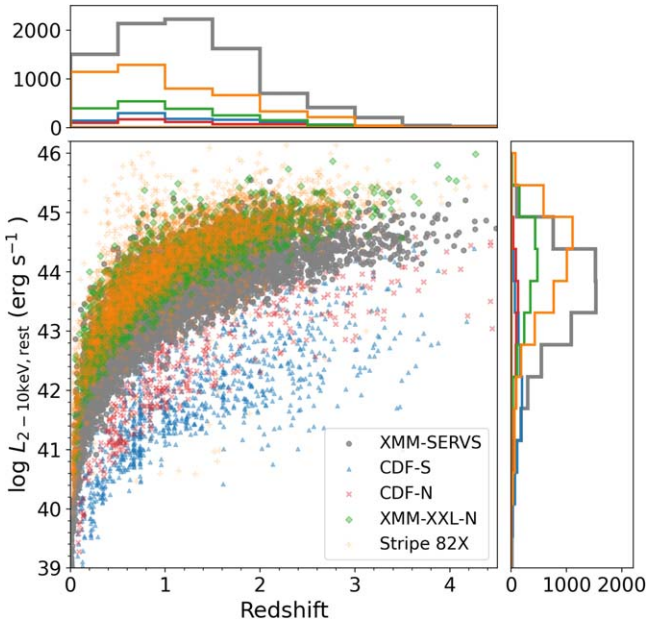

Figure 26. The $L_{2-10\ \mathrm{keV}}$ vs. z distribution of X-ray sources with spec-z or high-quality photo-z measurements in the full XMM-SERVS survey (gray circles). For comparison, the $L_{2-10\ \mathrm{keV}}$ vs. z distributions of X-ray sources in CDF-S (Luo et al. 2017), CDF-N (Xue et al. 2016), XMM-XXL North (e.g., Menzel et al. 2016), and Stripe 82X (e.g., Ananna et al. 2017; LaMassa et al. 2019) are shown as blue triangles, red crosses, green diamonds, and orange plus signs, respectively. The distributions of z for X-ray sources in the survey fields mentioned above are shown in the top subpanel, with colors the same as those in the legend; the distributions of $L_{2-10\ \mathrm{keV}}$ are shown in the right subpanel, with colors the same as those in the legend.

density, and $S_{1.4\ \mathrm{GHz,obs}}$ is the 1.4 GHz flux density). Among 213 objects in W-CDF-S and 86 objects in ELAIS-S1 that have both 24 μm and 1.4 GHz counterparts detected, 49/15 objects in W-CDF-S/ELAIS-S1 are identified as AGNs. A total of 14/0 of these objects in W-CDF-S/ELAIS-S1 are not already identified as AGNs via the first four methods.

The combination of all these methods identifies 3129 AGNs in W-CDF-S and 1957 AGNs in ELAIS-S1, which is ≈87%/86% of X-ray sources matched to multiwavelength counterparts with $p_{\mathrm{any}} > 0.1$. The non-AGN X-ray sources could be attributed to stars, bright galaxies (which can contain X-ray binaries and/or low-luminosity AGNs), and other source classes (see Appendix C).

7. Summary and Future Work

We have presented the X-ray point-source catalogs for two of the XMM-SERVS fields, W-CDF-S and ELAIS-S1, in this work. These are the final two fields of the ≈30 ks depth XMM-Newton survey, XMM-SERVS (≈13 deg^2 in total). The main results are the following:

1. 2.3 Ms and 1.0 Ms of XMM-Newton observations were performed in the ≈4.6 deg^2 W-CDF-S field and the ≈3.2 deg^2 ELAIS-S1 field, respectively. After background filtering, the median cleaned PN+MOS1+MOS2 exposure time is ≈84 ks in W-CDF-S and ≈ 80 ks in ELAIS-S1 (see Section 2). Our survey in W-CDF-S/ELAIS-S1 has a flux limit of 1.0×10^{-14} erg cm^{-2} s^{-1}/1.3×10^{-14} erg cm^{-2} s^{-1} over 90% of its area in the 0.5–10 keV band (see Section 3.6).
2. We compiled the X-ray point-source catalogs in W-CDF-S and ELAIS-S1 with the SAS task EMLDETECT. Adopting detection likelihoods that correspond to a spurious fraction of ≈1% (obtained through simulations; see Section 3.3), 4053 point sources are detected in W-CDF-S, and 2630 point sources are detected in ELAIS-S1. These X-ray sources have a median positional uncertainty of ≈1.″2 (see Section 3).
3. Utilizing optical-to-NIR data from DES, HSC, VOICE, VIDEO, and DeepDrill, we use NWAY to identify multiwavelength counterparts for X-ray sources in the catalogs. A total of 3600 (≈89%) X-ray sources in W-CDF-S and 2288 (≈87%) X-ray sources in ELAIS-S1 are matched to reliable optical and/or NIR counterparts (see Section 4).
4. Photometric redshifts are estimated for 3319/2001 X-ray sources in W-CDF-S/ELAIS-S1 with optical-to-NIR forced photometry available; type 1 AGNs are identified and fit separately with a suitable SED library. A total of 2752 X-ray sources in W-CDF-S and 1702 X-ray sources in ELAIS-S1 have either spectroscopic or high-quality ($\sigma_{\mathrm{NMAD}} \approx$ 0.03–0.04 for non-BL AGNs and $\sigma_{\mathrm{NMAD}} \approx$ 0.06–0.07 for BL AGNs when compared to spec-zs) photometric redshifts (see Section 5).
5. We identify 3129 X-ray sources in W-CDF-S and 1957 X-ray sources in ELAIS-S1 as AGNs based on their optical spectroscopic properties, X-ray luminosity and/or spectral shape, and X-ray-to-NIR SED template fitting results. MIR color and radio luminosity are also utilized to select AGNs when available (see Section 6).

The X-ray point-source catalogs provided in this work will have great legacy value for studies of AGNs across the full range of cosmic environments and will enable large-scale studies of SMBH growth in the multidimensional space of galaxy parameters. We note that all the XMM-SERVS fields, including W-CDF-S and ELAIS-S1, are selected LSST deep drilling fields, which will have ≈900 epoch *ugrizy* coverage with co-added depth reaching $i \approx 28$; the robustly identified X-ray AGNs will be useful for calibrating LSST AGN selection in the deep drilling fields and the main survey. Future deep radio coverage from MIGHTEE (e.g., Jarvis et al. 2016), submillimeter coverage from LMT and ALMA, and spectroscopic data from DEVILS, MOONS, and WAVES (e.g., Davies et al. 2018; Driver et al. 2019; Maiolino et al. 2020) will also contribute to the legacy value of the W-CDF-S and ELAIS-S1 fields. The SDSS-V Black Hole Mapper Program (Kollmeier et al. 2017) and the 4MOST TiDES Program (Swann et al. 2019) will provide direct SMBH masses for hundreds of the AGNs in these fields. Together with this superior multiwavelength coverage, the X-ray catalogs presented in this work will enable outstanding studies of the ≈5100 AGNs reported. We leave detailed characterization of extended X-ray sources in the XMM-SERVS fields for future work, which will contribute to the studies of X-ray groups and clusters (e.g., Pierre et al. 2016).